

A design of ILC E-driven positron source

M Kuriki¹, H Tajino¹, S Konno¹, Z Liptak¹, T Takahashi¹,
M Fukuda², T Omori², Y Seimiya², J Urakawa², K Yokoya²
and S Kashiwagi³

¹ Hiroshima U. ADSE, Higashihirosima, Japan

² KEK, Tsukuba, Japan

³ Tohoku U. ELPH, Sendai, Japan

E-mail: mkuriki@hiroshima-u.ac.jp

Abstract. ILC is an electron-positron linear collider based on Superconducting linear accelerator. Linear collider is the only solution to realize high energy electron-positron collision beyond the limit of synchrotron radiation energy loss by ring colliders. Beam current of injector of linear colliders is much larger than that of ring colliders because the beam is not reusable. Providing an enough amount of particles, especially positron is a technical issue. In this article, we present a design of electron driven positron source for ILC. After optimizations, the system design is established with an enough technical margin, e.g. avoiding potential damage on the production target.

1. Introduction

ILC is an e⁺e⁻ linear collider with center of mass energy 250 GeV - 1000 TeV [1]. It employs Super-conducting accelerator to boost up the beam up to the designed energy. The beam is accelerated in a macro pulse with 1300 bunches by 5 Hz repetition. The bunch charge is 3.2 nC resulting the average beam current 21 μ A. This is a technical challenge, because the amount of positron per second is 40 times larger than that in SLC [2], which was the first linear collider.

The configuration of the positron source is schematically shown in figure 1. The positron generated by electron beam is captured and boosted up to 5 GeV by two linacs. In the E-driven ILC positron source, the drive beam energy is 3.0 GeV and the target is 16 mm thick W-Re alloy rotating with 5 m/s tangential speed. FC (Flux Concentrator) generates a strong magnetic field to compensate the transverse momentum. 36 1.3 m L-band Standing Wave (SW) cavities with 0.5 Tesla solenoid field are placed for positron capture. This section is called as the capture linac. At the downstream, a chicane is placed to removes electrons. The positron booster is composed from 2.0 m L-and and 2.0 m S-band Traveling Wave (TW) cavities. ECS (Energy Compression Section) is composed from 3.0 m L-band TW cavities with chicane.

In E-driven ILC positron source, positrons are generated in a multi-bunch format as shown in figure 2. One RF pulse contains 66 bunches with 80 ns gap. To generate 1312 bunches for positrons of one RF pulse in the main linac, this pulse is repeated 20 times in 64 ms to mitigate the potential damage on the production target. The number of positrons in one RF pulse is 20 times less than those in one RF pulse in the main linac, the instantaneous heat load on the target is also 20 times less [3].



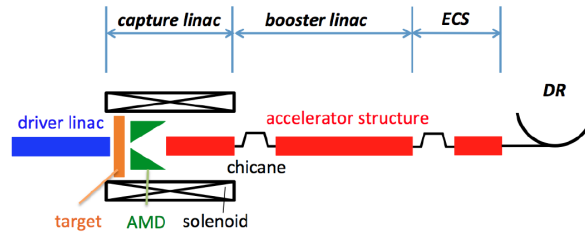


Figure 1. Configuration of E-driven ILC positron source is schematically shown.

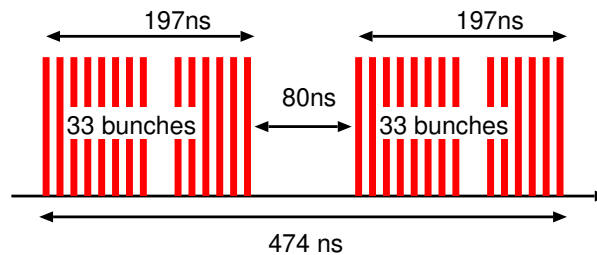


Figure 2. The beam structure in the positron source. Each mini-train contains 33 bunches.

A first simulation was performed by T. Omori [3] only for the capture linac. A simulation with the tracking down to DR (Damping Ring) was made by Y. Seimiya [4], but no beam loading effect was accounted. A new simulation with the beam-loading effect was done by Kuriki and Nagoshi [5,6]. For those simulations, the peak energy deposition density on the target is kept less than 35 J/g [7], which is considered to be a practical limit of the safety operation.

To obtain uniform intensity positrons over the pulse, the transient variation of the acceleration field by the beam loading has to be compensated so that positrons are accelerated uniformly. Compensation for the transient beam loading by Phase Modulation (PM) on the input RF was proposed by Urakawa [8,9]. The detail study of the compensation is discussed in Ref. [10,11]. In this article, we present the electron driven ILC positron source accounting this effect.

2. Subsystems

2.1. Electron driver

3 GeV electron driver is composed from 2600 MHz (S-band) normal conducting TW cavity. The cavity is originally designed for ATF (Accelerator Test Facility) at KEK [12] in 2856 MHz and the parameters are scaled to 2600 MHz. 4 cavities are driven by two klystrons. Accounting 10 % power loss in RF wave guide, the input power to one cavity is 36 MW. The shunt impedance is 57.2 M Ω /m with L=3.228 m and the attenuation τ is 0.57 resulting 0.91 μ s filling time. The beam loading compensation was performed by amplitude modulation (AM) [11]. The acceleration voltage per cavity is 31.9 ± 0.4 MV with 0.65 A beam loading current I_B with 36 MW input power [11]. The first two cavities are driven by two klystrons, so that the input power per cavity is 72 MW resulting 43.5 ± 0.6 MV with the same I_B . The electron driver is composed from two cavities as the injector and 100 cavities as the normal section. The total beam energy is 3.3 GeV which has 10% margin.

AM and PM are employed to compensate the beam loading. These modulation on the input RF is made by mixing two RF inputs with PM on the low level RF. The detail is expressed in Ref. [11].

2.2. Target and magnetic focusing

Target is 16 mm tungsten-rhenium alloy. To avoid overlapping of the pulse on the target, it is rotated with 5 m/s tangential speed. At the down stream of the target, a flux concentrator as a magnetic focusing to suppress the transverse momentum is placed. The detail of those arrangements is presented in Ref. [6]. The loading on the target is evaluated by PEDD (Peak Energy Deposition Density in J/g); the W-Re destruction limit is 76 J/g [13], and the safe operating threshold is considered to be 35 J/g [6]. The positron production yield is 1.17 as evaluated in 3, the electron bunch charge is 4.1 nC. PEDD for 4.8 nC electron bunch is 33.6 J/g [6], giving 28.7 J/g for 4.1 nC. This is even lower the threshold.

2.3. Capture linac

The capture linac is composed from 36 APS (Alternate Periodic Structure) $\pi/2$ mode SW cavity. The structure is 1.3 m with 21 cells. The shunt impedance is 31.5 M Ω /m. The purpose of the capture linac is to confine the generated positrons in a RF bucket. An effective way for the capturing is the deceleration capture method where positrons are placed on the deceleration phase [14]. The positron is moving to the acceleration phase by phase slipping gradually and the positron is fixed at the acceleration phase. Figure 3 shows the captured positron distribution in the longitudinal phase space z and $\delta = (\gamma - \bar{\gamma})/\bar{\gamma}$ where γ and $\bar{\gamma}$ are Lorentz factor and the average. The positrons after acceleration are distributed along the RF curvature.

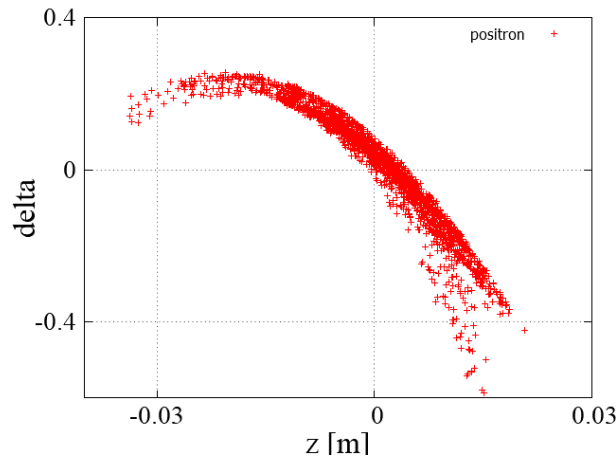


Figure 3. Longitudinal phase space ($z - \delta$) distribution of positron at the end of the capture linac.

The acceleration voltages induced by the input RF and the beam (beam loading voltage) are off-phase with a finite angle, θ in the capture linac. Due to the phase, the beam loading compensation by adjusting the timing doesn't work, because the cancellation between the growth of voltage by RF and voltage by beam is impossible. Instead of the timing adjustment, we employ PM on the input RF. General voltage evolution of SW cavity V is given as

$$\frac{dV(t)}{dt} = -\frac{(1 + \beta)\omega}{2Q} [V(t) - V_{BL}u(t - t_b) - V_{RF}u(t)] \quad (1)$$

where β is coupling to the cavity, Q is Q value, ω is angular frequency, V_{RF} and V_{BL} are the asymptotic voltages by RF and beam, $u(t)$ is a step function. The RF feed is started at $t = 0$ and the acceleration is started at $t = t_b$. Be careful those voltages are complex numbers in general. To obtain an uniform acceleration, the following condition has to be satisfied,

$$V(t_b) - V_{BL} - V_{RF} = 0. \quad (2)$$

If V_{BL} and V_{RF} are in different phases, this condition is never satisfied because $V(t_b)$ and V_{RF} are in phase. PM on V_{RF} is necessary to achieve this as,

$$V_{RF'} = V(t_b) - V_{BL} \quad (3)$$

where $V_{RF'}$ is the asymptotic value of the input RF after PM. V_{t_b} is minimized when $\theta = \pi$ which corresponds to crest acceleration. The maximum beam loading current is expected to be 2.0 A according to a simulation. By assuming 22.5 MW RF input and $\beta = 5$, $V_{RF} = 22.6$ MV and $V_{BL} = 13.7$ MV are expected giving 8.9 MV as the lowest acceleration voltage for each cavity. The total energy after the capture cavity is at least 320 MeV which has an enough margin comparing to the design energy 250 MeV.

2.4. Chicane and booster linac

After the capture linac, a chicane is placed to remove electrons. As a sub-effect, the bunch length is shortened by the momentum compaction factor. The chicane parameter is adjusted as the bunch length after the chicane is minimized as shown in figure 4.

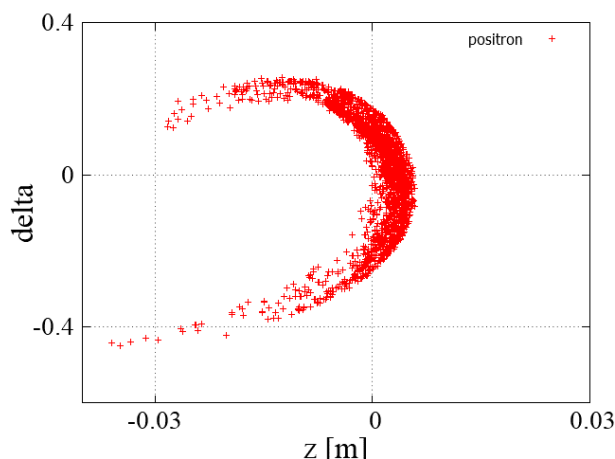


Figure 4. Longitudinal phase space ($z - \delta$) distribution of positron after the chicane.

The positron booster is composed from L-band [15] and S-band [16] Traveling Wave (TW) cavities. The parameters are summarized in table 1.

Table 1. Parameters of L-band and S-band TW cavities in the booster.

Parameter	L-band	S-band	unit
Shunt impedance	46.5	55.1	MΩ/m
Length	2.00	1.96	m
Aperture (2a)	35.0 39.4	24.3-20.3	mm
Attenuation τ	0.261	0.333	
Filling time t_f	1.28	0.55	μ s

Beam loading compensation method is different from that for the capture linac. It is compensated with AM on the input RF [10]. According to Ref. [10], a perfect compensation is possible with two components AM, i.e. AM with a step pulse and a trapezoidal pulse. In this

design study, we employ one component AM with a step pulse. E_0 is the initial cavity field, and E_1 is the amplitude of AM. E_1 is determined as

$$E_1 = \frac{rI}{2} \left(\frac{-\omega/Qt_p e^{-2\tau}}{1 - e^{-\omega/Qt_p}} + 1 \right), \quad (4)$$

where t_p is the pulse length. The cavity voltage is same at $t = t_f$ and $t = t_f + t_p$. The initial field E_0 is determined as

$$P_{max} = \frac{L}{r(1 - e^{-2\tau})} (E_0 + E_1)^2 \quad (5)$$

where P_{max} is the maximum input RF power.

By assuming 4.8 nC bunch charge, the beam loading current in the booster is 0.78 A. The acceleration voltage per cavity is evaluated as 16.5 ± 0.1 MV for L-band cavity and 29.2 ± 0.6 MV for S-band cavity. Those voltages are evaluated with P_{max} is 22.5 MW for L-band and 36 MW for S-band including 10% power loss by wave guide. Table 2 summarizes the lattice configuration of the booster based on the design in Ref. [4]. As the energy at the booster entrance, 250 MeV is assumed.

Table 2. Lattice configuration of the booster. 4Q+1L means the lattice is composed from four quadrupoles and one L-band cavity, etc. Energy gain is the acceleration energy in the section and Energy is the beam energy at the end of the section in MeV.

Lattice	unit #	# of cavity	Energy gain	Energy
4Q+1L	3	12	198	448
4Q+2L	15	60	990	1438
4Q+4L	18	72	1188	2626
4Q+4S	25	100	2860	5486

2.5. Energy compression section

The purpose of ECS to compress the energy spread of positron after the booster, down to $\pm 0.75\%$, within DR (damping ring) acceptance. ECS is composed from three chicane (18.6m, 55.8 m in total) and 4 L-band 3m TW cavities (4Q+4L lattice, 22.4 m) driven by 4 klystrons. Other two L-band 3m TW cavities (2L, 6.4 m) driven by two klystrons are set for the beam loading compensation.

3. Positron yield evaluation

The positron yield is defined as the number of positrons obtained in DR dynamic aperture (acceptance) per electrons on the production target. The DR acceptance is [1]

$$\gamma A_x + \gamma A_y < 0.07 \text{ m}, \quad (6)$$

$$\left(\frac{z}{0.035 \text{ m}} \right)^2 + \left(\frac{\delta}{0.0075} \right)^2 < 1.0. \quad (7)$$

Figure 5 shows the longitudinal phase space distribution after ECS with DR acceptance (solid circle). Figure 6 shows positron yield as a function of R_{65} of ECS. R_{56} is optimized for each R_{65} . Yield is 1.17 and uniform in region of $-1.2 < R_{65} < -1$.

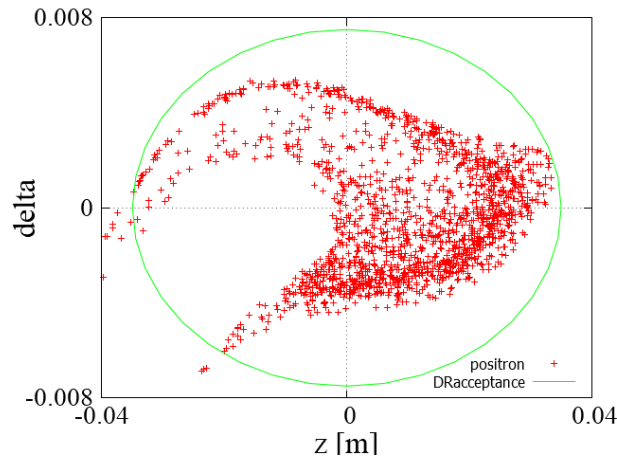


Figure 5. Longitudinal phase space ($z - \delta$) distribution of positrons after ECS section. R_{56} of ECS is -1.04. The solid circle shows DR acceptance.

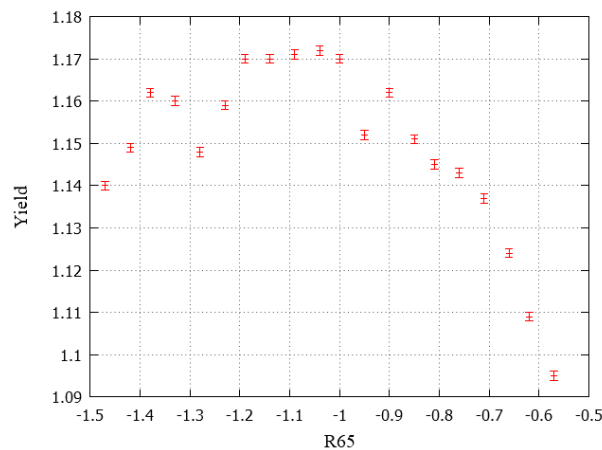


Figure 6. Positron yield as a function of R_{65} of ECS. R_{56} is optimized for each R_{65} . Yield is uniform $-1.2 < R_{65} < -1$.

4. Summary

According to detail studies of the beam loading compensation for SW and TW cavities, the acceleration field is determined. Based on those parameters, the number of RF units and the lattice are fixed and the ILC E-driven positron source design is established. The evaluated positron yield was 1.17 giving the electron intensity on the target satisfying the safety condition.

Acknowledgments

This work is partly supported by Grant-in-Aid for Scientific Research (B) and US-Japan Science and Technology Cooperation Program in High Energy Physics.

References

- [1] ILC collaboration 2013 ILC Technical Design Report Tech. rep. KEK-Report
- [2] SLC Design Report Tech. rep. SLAC-R-714, 1984
- [3] Omori T *et al.* 2012 *Nucl. Instrum. Methods Phys. Res., Sect. A* **672** 52
- [4] Seimiya Y *et al.* 2015 *Prog. Theor. Exp. Phys.* **2015** 103G01
- [5] Kuriki M *et al.* 2016 in *Proc. 28th Linear Accelerator Conf. (LINAC'16)* (East Lansing, MI USA) pp 430–33

- [6] Nagoshi H and Kuriki M *et al.* 2019 *Nucl. Instrum. Methods Phys. Res., Sect. A* **953** 163134
- [7] Takahashi T 2018 *Proc. of Int. Workshop on Future Linear Colliders (LCWS2018)* (Arlington, Texas USA)
- [8] Kuriki M *et al.* 2021 *Proc. 12th Int. Particle Accelerator Conf. (IPAC'21)* (Campinas, Brazil) pp 1368–71
- [9] Kuriki M *et al.* 2021 *Proc. 18th annual meeting of Particle Accelerator Society of Japan (PASJ2021)* (Takasaki, Japan) pp 315–19
- [10] Kuriki M 2018 *Proc. 9th Int. Particle Accelerator Conf. (IPAC'18)* (Vancouver, Canada) pp 307–10
- [11] Kuriki M *et al.* 2022 *Proc. 13th Int. Particle Accelerator Conf. (IPAC'22)* (Bangkok, Thailand) pp 1893–96
- [12] ATF Design and study report Tech. rep. KEK Internal 95-4, 1995
- [13] Ecklund S 1981 Positron target materials tests Tech. rep. SLAC-CN-128
- [14] James M *et al.* 1991 *Nucl. Instrum. Methods Phys. Res., Sect. A* **307** 207
- [15] Saito K *et al.* 2010 *Proc. 7th annual meeting of Particle Accelerator Society of Japan (PASJ2010)* (Himeji, Japan) pp 532–36
- [16] Matsumoto S, Higo T, Kakihara K, Kamitani T and Tanaka M 2014 *Proc. 5th Int. Particle Accelerator Conf. (IPAC'14)* (Dresden, Germany) pp 3872–74